Hypoxia inducible factor 1α contributes to regulation of autophagy in retinal detachment

Shameka J. Shelby[a], **Pavan S. Angadi**[a], **Qiong-Duon Zheng**[a], **Jingyu Yao**[a], **Lin Jia**[a], and **David N. Zacks**[a,*]

[a]Department of Ophthalmology and Visual Sciences, University of Michigan Medical School, 1000 Wall St, Ann Arbor, Michigan, 48105-0714, USA

Abstract

Photoreceptor (PR) cells receive oxygen and nutritional support from the underlying retinal pigment epithelium (RPE). Retinal detachment results in PR hypoxia and their time-dependent death. Detachment also activates autophagy within the PR, which serves to reduce the rate of PR apoptosis. In this study, we test the hypothesis that autophagy activation in the PR results, at least in part, from the detachment-induced activation of hypoxia-inducible factors (HIF). Retina-RPE separation was created in Brown-Norway rats and C57BL/6J mice by injection of 1% hyaluronic acid into the subretinal space. Retinas were harvested and assayed for HIF protein levels. Cultured 661W photoreceptor cells were subjected to hypoxic conditions and assayed for induction of HIF and autophagy. The requirement of HIF-1α and HIF-2α in regulating photoreceptor autophagy was tested using siRNA in vitro and in vivo. We observed increased levels of HIF-1α and HIF-2α within 1 day post-detachment, as well as increased levels of BNIP3, a downstream target of HIF-1α that contributes to autophagy activation. Exposing 661W cells to hypoxia resulted in increased HIF-1α and HIF-2α levels and increase in conversion of LC3-I to LC3-II. Silencing of HIF-1α, but not HIF-2α, reduced the hypoxia-induced increase in LC3-II formation and increased cell death in 661W cells. Silencing of HIF-1α in rat retinas prevented the detachment-induced increase in BNIP3 and LC3-II, resulting in increased PR cell death. Our data support the hypothesis that HIF-1α, but not HIF-2α, serves as an early response signal to induce autophagy and reduce photoreceptor cell death.

Keywords

Retinal detachment; hypoxia-inducible factor; photoreceptors; autophagy; hypoxia

---

*To whom correspondence should be addressed: University of Michigan Medical School, Kellogg Eye Center, 1000 Wall Street, Ann Arbor, MI 48105-0714; davzacks@med.umich.edu.

1. Introduction[1]

Photoreceptor (PR) cells, the visual sensing elements of the retina, obtain their nutritional and metabolic support from the underlying retinal pigment epithelium (RPE). These two cell types interact intimately on the structural level, with microvilli on the apical surface of the RPE surrounding the photoreceptor outer segments (Ban and Rizzolo, 2000; Strauss, 2005). Separation of the retina from the RPE can lead to devastating consequences for the photoreceptor cells and the remainder of the neural retina (Piccolino et al., 2005). This separation occurs commonly, either alone as a retinal detachment or as part of a larger clinical problem (Burton, 1982).

Despite improved techniques for reattaching the retina to the RPE, visual recovery is often compromised, and this loss of vision is primarily due to the death of the photoreceptor cells (Cook et al., 1995; Hisatomi et al., 2002; Zacks et al., 2003). Previous work from our laboratory has identified the involvement of Fas mediated apoptosis in photoreceptor cell death following retinal detachment. This well-defined death receptor is activated after detachment and results in downstream activation of the apoptotic cascade (Zacks et al., 2007; Zacks et al., 2004). Paradoxically, not all photoreceptors die immediately when separated from the RPE, despite the fact that the former are dependent upon the latter for the majority of their metabolic needs. It is well known that there is a clinical "window-of-opportunity" to reattach the retina to the RPE and obtain useful visual recovery (Ross, 2002; Ross and Kozy, 1998; Ross and Stockl, 2000). This suggests that intrinsic anti-apoptotic, or pro-survival pathways, become activated post-detachment and serve to counteract or mitigate the activation of Fas mediated apoptosis. Additional work from our laboratory has identified such pro-survival pathways that become activated, including the interleukin-6 pathway and the autophagy pathway (Besirli et al., 2011; Chong et al., 2008).

Photoreceptor hypoxia occurs upon separation of the retina from the RPE (Linsenmeier, 1990; Mervin et al., 1999). Major regulators of cellular response to decreased oxygen are the Hypoxia Inducible Factors (HIF) (Bellot et al., 2009; Mazure and Pouyssegur, 2010; Rouschop and Wouters, 2009). HIFs are heterodimeric transcription factors that are made up of α and β subunits, both of which are constitutively expressed. Under normoxic conditions, HIFα is marked for degradation by Prolyl Hydroxylase Domain (PHD) and Factor Inhibiting

---

1

Abbreviations

PR   photoreceptors

RPE   retinal pigment epithelium

HIF   hypoxia inducible factors

PHD   prolylhydroxyl domain

FIH   factoring inhibiting HIF

BNIP3   Bcl-2/E1B 19 kDa-interacting protein 3

HIF (FIH) proteins. When oxygen tension is reduced, PHD and FIH are inactivated allowing for the persistence of HIFα in the cytoplasm (Brahimi-Horn and Pouyssegur, 2009; Jiang et al., 1996; Kong et al., 2007; Wang et al., 1995; Wang and Semenza, 1995). The HIF family consists of three isoforms including HIF-1, HIF-2, and HIF-3. HIF-1 and HIF-2 are known to function in the activation of hypoxia dependent transcription, while the function of HIF-3 is not well understood (Benita et al., 2009; Greer et al., 2012; Li et al., 2006). Given that HIFs are transcription factors, their increased levels can result in significant activation of stress response and other pro-survival genes (Benita et al., 2009; Brahimi-Horn and Pouyssegur, 2009). In some disease models, HIF signaling results in increased levels of BH3-only protective protein – Bcl-2/E1B 19 kDa-interacting protein 3 (BNIP3), a protein that protects the cell from cell death during damage by activation of autophagy (Mazure and Pouyssegur, 2010; Pouyssegur et al., 2006).

In this study, we test the hypothesis that autophagy activation in the PR results, at least in part, from the detachment-induced activation of HIF. We use our established model of retinal detachment and in vitro studies using the 661W photoreceptor cells to identify the role of hypoxia in induction of autophagy after retinal detachment. Our findings suggest that the hypoxic environment of the photoreceptors during retinal detachment increases the levels of both HIF-1α and BNIP3, resulting in increased autophagy and cell survival.

2. Methods

2.1. Animals

Experimental procedures involving animals were performed in accordance with the guidelines and under the approval of the University Committee on Use and Care of Animals at the University of Michigan, and were in compliance with the statement for ethical care and use of animals of the Association for Research in Vision and Ophthalmology (ARVO). Brown-Norway rats were obtained from Charles River Laboratories. C57BL/6J mice were obtained from Jackson Laboratories. Rats and mice were housed in a 12-h/12-h light-dark cycle. Surgeries were performed on animals sedated with a ketamine and xylazine mixture. All animal experiments contained at least three rats or mice per group and were performed a minimum of three times.

2.2. Experimental Model of Retinal Detachment

Retinal detachments were created in adult Brown-Norway rats and C57BL/6J mice as previously described using hyaluronic acid to prevent reattachment (Verardo et al., 2008; Zacks et al., 2003). All detachments were created in the left eye with the right eyes serving as attached controls in 3 month old male mice or 6 month old male rats. For siRNA treatments, 5 μL of 1X siRNA buffer (Thermo Scientific, Hanover Park, IL, USA) containing 0.5×10^{-9} moles of ON-TARGETplus SMARTpool HIF-1α siRNA (siHIF-1α) or ON-TARGETplus Non-Targeting Pool (siControl) (Thermo Scientific) were introduced into the subretinal space following the creation of the detachment.

2.3. Cell Culture and siRNA treatment

The 661W photoreceptor cell line, a validated murine cone-derived cell line, was a gift from Dr. Muayyad Al-Ubaidi (Department of Cell Biology, University of Oklahoma Health Sciences Center, Oklahoma City, OK, USA) (al-Ubaidi et al., 1992; Al-Ubaidi et al., 2008). 661W cells were maintained in DMEM supplemented with 10% fetal bovine serum (FBS), 1 mM penicillin/streptomycin, 300 mM L-glutamine, 32 mM putrescine, 40μL/L β-mercaptoethanol, 40 μM hydrocortisone 21-hemisuccinate, and 40 μM progesterone at 37°C in 5% CO2. Mouse and rat HIF-1 α and HIF-2α siRNAs were obtained as Smartpools (Thermo Scientific) containing mixtures of four different duplexes to minimize silencing of unintended targets. ON-TARGET plus non-targeting siRNA (at the same concentration as the total pool of targeting siRNAs) served as a negative control. 661W were passaged into eight-well chamber slides or 12 well plates, and 24 h later each well was transfected with 0.33 μg or 1.32 μg of the siRNAs plus 1.25 μL or 5 μL of DharmaFect 3 transfection reagent (Thermo Scientific). The cells were incubated with the siRNAs for 48 h. Cell viability was assessed by trypan blue staining, and was nearly equivalent in cultures treated with targeting and non-targeting siRNAs.

2.4. Hypoxia Assays

For experiments performed in hypoxic conditions, culture dishes were incubated for various times at 37°C in a modular incubator ch amber (Billups-Rothenberg, Inc, Del Mar, CA, USA) containing humidified hypoxic air (1% O_2, 5% CO_2, 94% N_2). The chambers were flushed frequently with hypoxic air to ensure maintenance of oxygen levels.

2.5. Caspase and Cell Viability Assays

Caspase 8 activity was measured using the luminescent tetrapeptide cleavage assay kit (Promega Corporation, Madison, WI, USA). 661W cells were cultured as above in 96-well plates with siRNA treatment. Cells were subsequently subjected to hypoxic conditions and Caspase 8 activity was measured at times indicated by incubating the cells with the substrate and measuring luminescence with a luminometer.

2.6. Antibodies and Reagents

The primary antibodies used were: HIF-1α (R&D Systems Inc., and Minneapolis, MN, USA); HIF-2α (Thermo Scientific); LC3 (Cell Signaling Technology, Boston, MA, USA); LC3-B (Novus Biologicals, Littleton, CO, USA); GAPDH (Ambion, Hanover Park, IL, USA); β-actin and BNIP3 (Abcam, Cambridge, MA, USA). AlexaFluor 555-conjugated anti-rabbit IgG, AlexaFluor 488-conjugated anti-rabbit IgG, AlexaFluor 555-conjugated anti-mouse IgG, anti-GFP 488, and Sybr safe were from Invitrogen (Carlsbad, CA, USA). Complete protease inhibitors and AmpliTaq Gold polymerase were from Roche Diagnostics (Indianapolis, IN, USA). RNeasy kit, Superscript III, and oligo-dT were from Qiagen (Valencia, CA, USA). All other reagents were from Sigma-Aldrich (St. Louis, MO, USA).

2.7. Western Blot Analysis

Retinas were dissected from animals with experimental detachments and control animals at various time points. The tissues were homogenized in 20 mM MOPS, 2 mM EGTA, 5 mM

EDTA, 1% Triton-X-100, 1 mM DTT, plus protease inhibitors. 661W cells were lysed and homogenized in the same hypotonic lysis buffer. For both tissue types, the cellular debris was removed by low speed centrifugation and protein concentrations of supernatants were determined by modified Lowry assay (Peterson, 1977). Protein samples were separated by SDS-PAGE, transferred onto Polyvinylidene difluoride membranes that were blocked, incubated with primary antibody, washed, and incubated with horse radish peroxidase-conjugated secondary antibody, developed with 3,3'-diamino denzidine, and exposed to film. Immunolabeling of LC3-II was quantified by densitometry and comparison to LC3-I or GAPDH (Barth et al., 2010).

2.8. Quantitative Real Time Polymerase Chain Reaction (qRT-PCR)

Total RNA was isolated from dissected rat retinas using RNAeasy kits, and first-strand cDNAs were synthesized using Superscript III and oligo-dT. Sequences encoding HIF-1α were amplified with gene-specific primers forward 5'-TCCATGTGACCATGAGGAAA-3' and reverse 5'-GAGGCTGTGTCGACTGAGAA-3', which flanks one intron in the genomic sequence using AmpliTaq Gold polymerase in the presence of Sybr green (Applied Biosystems, Foster City, CA, USA). Primers for hypoxanthine-guanine phosphoribosyltransferase (Hprt) forward 5'-GCAGACTTTGCTTTCCTTGG-3'; reverse 5'-CCGCTGTCTTTTAGGCTTTG-3' served as a control. PCR for validation of knockdown in 661W cells was performed using the following primers specific for the following murine sequences: Hif-1α forward 5'-TCCATGTGACCATGAGGAAA-3'; reverse 5'-GAGGCTGTGTCGACTGAGAA-3'; Hif-2α forward 5'-AATCTGAAGCTGAGGCCGAC-3'; reverse 5'-TTCCCAAAACCAGAGCCGTT-3'; Gapdh forward 5'-TGTCCGTCGTGGATCTGA-3'; reverse 5'-CCTGCTTCACCACCTTCTTG-3'.

2.9. Immunohistochemistry

Detachments were performed in C57BL/6J mice, GFP-LC3 mice, and Brown Norway rats and eyes fixed with 4% paraformaldehyde, washed with PBS, transitioned to sucrose/OCT, and flash frozen. Retinal cross sections (10 μm) were washed with PBS and permeabilized with PBS-T (0.3% Triton X-100); blocked with 1% bovine serum albumin, 10% normal goat serum, and 0.3% Triton X-100; and incubated with primary antibodies for 2 h, then with fluorophore-conjugated secondary antibodies for 1 h. Species and dilutions of primary antibodies were as follows: Mouse anti-HIF-1α (1:150), anti-BNIP3 (1:200); Rabbit anti-HIF-2α (1:100), anti-LC3B (1:150). Secondary antibodies used were AlexaFluor 488 anti-rabbit IgG (1:1500); AlexaFluor 488 anti-mouse IgG (1:1500); AlexaFluor 555 anti-rabbit IgG (1:1500), and anti-GFP 488. Sections were counterstained with ProLong Gold with 406-diamidino-2-phenylindole (DAPI; Invitrogen) to reveal cell nuclei. Stained sections were imaged using a Leica DM6000 fluorescence microscope. For immunohistochemistry with 661W cells, the cultures were subjected to hypoxic conditions, washed 3 times with PBS, and fixed with 4% paraformaldehyde for 30 min at room temperature. The cells were then processed using the same methods as for retinal cross sections. The number of autophagosomes in 661W cells subjected to hypoxic conditions or normoxic controls were quantified by counting punctae in cells stained with LC3B antibody. 9 non-overlapping areas of 100μm (containing approximately 50 cells each) were counted for each condition to

determine the average number of LC3 punctae per cell. Data are represented as mean ± SE (*n* = 9 per group). Images shown are representative of a minimum of 3 trials.

2.10. TUNEL Staining

At 72 hours post detachment and treatment with siRNA, animals were euthanized and the eyes were enucleated. For TUNEL staining, whole eyes were fixed with 4% paraformaldehyde, embedded in paraffin, and sectioned at a thickness of 6 μm. TUNEL staining was performed on the sections using ApopTag Fluorescein In-Situ Kit (Millipore). TUNEL-positive cells in the outer nuclear layer were quantified from high magnification images of 9 non-overlapping regions of 300 μm each. A minimum of 3 animals were used for each condition.

2.11. Statistical Analysis

Data sets were analyzed by comparing groups with a two-tailed Student's t-test or analysis of variance (ANOVA) followed by Bonferroni post hoc analysis where appropriate. Differences were considered significant at $p < 0.05$.

3. Results

3.1. Retinal detachment increases HIF-1α and HIF-2α protein levels

Light microscopic analysis of a mouse retina 1 day post experimental detachment demonstrated the stability of the detachments (Fig. 1A). Analysis of protein levels on western blots of detached mice and rat retinas showed a marked increase in the level of HIF-1α and HIF-2α protein at 1 day post-detachment that decreased at 3 days (Fig. 1B, C). Immunohistochemical analysis confirmed the presence of HIF-1α and HIF-2α expression in photoreceptor inner and outer segments at 1 day post-detachment (Fig. 1D).

3.2. BNIP3 expression and autophagy activation after retinal-detachment

Under hypoxic conditions, HIF-1α can induce a cell survival response through the induction of BNIP3 expression, a protein that competes with Bcl-2 and Bcl-XL to release beclin and stimulate autophagy (Bellot et al., 2009; Maiuri et al., 2007; Mazure and Pouyssegur, 2009; Tracy et al., 2007; Zhang et al., 2008). Western blot analysis of lysates from attached and detached retinas showed increased BNIP3 expression at 1 and 3 days post-detachment in mice and rats (Fig. 2A, B). Conversion of LC3-I to LC3-II, a standard measure of autophagy activation (Mizushima et al., 2010), peaked at 1 day post-detachment and remained at 3 days in mice (Fig. 2A). LC3-II peaked at 1 day post-detachment, while a decrease was seen at 3 days in rats (Fig. 2B), consistent with increased autophagy flux as previously demonstrated (Besirli et al., 2011). Immunohistochemical analysis of retinas with antibody against BNIP3 showed localization in the inner segment of the photoreceptor at 1 day post-detachment (Fig. 2C). The appearance of staining at the distal tips of PR outer segments is likely from secondary autofluorescence in the degenerating outer segments. Sections from GFP-LC3 mice showed punctate staining in the inner segments, corresponding to the increased conversion of LC3-I to LC3-II and increased autophagosome formation at 1 day following detachment (Fig. 2D white arrows) (Mizushima et al., 2010). These results indicate that the expression of BNIP3 and LC3 in detached rat retinas correlates with HIF levels.

3.3. Hypoxia in 661W cells leads to increased HIF-1α and HIF-2α protein levels

To directly assess the involvement of HIF-1α and HIF-2α in hypoxia-mediated autophagy in retinal detachment, we created an in vitro system to mimic the in vivo condition adopted from established protocols (Wu and Yotnda, 2011). Previous studies in our lab have utilized 661W cells, an immortalized mouse cone-like photoreceptor cell line (al-Ubaidi et al., 1992; Besirli et al., 2010, 2011; Besirli et al., 2012; Tan et al., 2004). In the current study, we utilized a modular incubator chamber containing humidified hypoxic air (1% O_2, 5% CO_2, 94% N_2) to create hypoxic conditions for the 661W cells. We first assessed whether this hypoxic air mixture was sufficient for induction of HIF-1α and HIF-2α protein expression in 661W cells. Western analysis showed both HIF-1α and HIF-2α were present in homogenates of 661W cells incubated in hypoxic conditions from 2 hours to 48 hours (Fig 3A). Immunostaining of cultured cells incubated in hypoxic conditions for 24 hours also demonstrated an increase in nuclear staining over the control, normoxic samples, which exhibited minimal levels of HIF-1α and HIF-2α (Fig. 3B).

3.4. Hypoxia induces autophagy in 661W cells

We next sought to determine whether autophagy is activated, at least in part, in response to hypoxia in 661W cells. Following incubation in hypoxic conditions, LC3-I to LC3-II conversion appeared to peak at 16 hours, and decrease at later time points. Western analysis also showed that BNIP3 levels increased early after induction of hypoxia (Fig. 4A). To further confirm that hypoxia leads to increased autophagy in photoreceptor cells, 661W cells incubated in hypoxic conditions were subjected to immunofluorescence microscopy using antibody against LC3B. Analysis of average puncta per cell demonstrated a marked increase of LC3 puncta over normoxic samples that increased with time (Fig. 4B). The contrast in detection of LC3 using immunoblotting and immunocytochemistry after 16 hours hypoxia suggested that hypoxia can induce autophagic flux. To determine whether this phenomenon was occurring in hypoxic 661W cells, cultures were incubated with Bafilomycin A1 (Baf A), an inhibitor of autophagosome-lysosome fusion (Sarkar et al., 2007), during the last 4 hours of hypoxic conditions for 24 hours (Fig. 4C). Western analysis of LC3 and p62 showed marked increase of both proteins with the addition of Baf A (Fig. 4C). These results demonstrate that hypoxic 661W cells which express HIF-1α and HIF-2α can initiate an autophagic response with increased autophagic flux.

3.5. Reduced HIF-1α expression decreases hypoxia-induced autophagy in 661W cells

To evaluate the effect of HIF-1α loss-of-function on hypoxia-induced autophagy, siRNAs were used to deplete HIF-1α transcripts in sub-confluent 661W photoreceptor cells, followed by incubation in hypoxic conditions for 16 and 24 hours. Transfection of 661W cells with a pool of four HIF-1α targeting siRNAs resulted in efficient knockdown at both the transcript and protein level (Fig. 5A, B). HIF-1α expression was retained in cells transfected with a pool of control non-targeting siRNAs. Equivalent levels of HIF-2α and GAPDH were present in both treated and control cells. Western analysis of HIF-1α silenced and non-targeting control cells incubated in hypoxia for 16 hours revealed decreased levels of BNIP3 and LC3-II (Fig. 5B). Immunocytochemical analysis of LC3B punctae demonstrated a significant decrease of approximately 50% in cells treated with HIF-1α

siRNAs in contrast to cells treated with control siRNAs when incubated in hypoxic conditions for 24 hours (Fig. 5C). Additionally, caspase 8 assays on cells with silencing of HIF-1α and incubated in hypoxic conditions showed a time dependent increase (p <0.0005). Cell viability assays also indicated that cell death increases in the presence of siHIF-1α (Fig. 5D). Note that in cultured cells, the LC3-I levels exhibit much more variability that may not truly be reflective of autophagy levels but of their cultured state. For this reason, in cultured cells we compare LC3-II levels (which are reflective of autophagy status) to GAPDH loading controls. This allows us to have a more definitive measurement of autophagy activity at each time point without comparing it to the highly variable LC3-I levels.

3.6. HIF-2α is not required for hypoxia-induced autophagy in 661W cells

To identify whether HIF-2α is also involved in hypoxia-induced autophagy in 661W cells, we used cells treated with siRNAs against HIF-2α. Transcript and protein levels of HIF-2α confirmed knockdown in 661W cells (Fig. 5E, F). In contrast to silencing of HIF-1α, knockdown of HIF-2α did not appear to effect the expression of BNIP3 or conversion of LC3-I to LC3-II (Fig. 5F). Immunohistochemical analysis and quantification of LC3 punctae confirmed the minimal effect of silencing HIF-2α on hypoxia-induced autophagy in 661W cells (Fig. 5G). Analysis of caspase 8 activity and cell viability demonstrated that silencing HIF-2α does not have a significant effect on activation of apoptosis (Fig. 5H). Taken together, these results demonstrate that hypoxia-induced autophagy in cultured photoreceptor cells is mediated by HIF-1α and not by HIF-2α.

3.7. Reduced HIF-1α expression in detached retinas decreases autophagy and increases cell death

To confirm results yielded from our cell culture model under hypoxic conditions, we used siRNA against HIF-1α in our rat retinal detachment model. A single dose of siHIF-1α or non-targeting control pool was injected into the subretinal space at the time of retina–RPE separation and animals were sacrificed 1 day post-detachment. Transcript expression was evaluated by quantitative real-time PCR and demonstrated a significant decrease in HIF-1α in siHIF-1α injected animals (p <0.005) (Fig. 6A). Knockdown of HIF-1α resulted in reduction of HIF-1α, LC3-II, and BNIP3 protein levels at 1 day post-detachment in stark contrast to animals injected with non-targeting control (Fig. 6B). Staining for LC3 showed punctate staining in the inner segments of rats injected with non-targeting control at 3 days following detachment in contrast to rats injected with siHIF-1α, which had very little punctate staining (Fig. 6C white arrows). In addition, silencing of HIF-1α in detached retinas showed an increase in TUNEL-positive cells at 3 days post detachment over non-targeting control (p<0.0005) (Fig. 6D). Taken together, these results confirm that silencing of HIF-1α in hypoxic 661W cells and animals with retinal detachments decreases autophagic response and increases cell death.

4. Discussion

Separation of the retina from the RPE results in significant disruption of photoreceptor homeostasis, and can eventually lead to death of these cells. This outcome, however, is not immediate and is regulated by a complex set of molecular events that serve to maintain cell

survival for a period of time after detachment. We have previously shown that Fas-mediated apoptosis is the major pathway driving photoreceptor death after detachment (Zacks et al., 2007; Zacks et al., 2004). We have also shown that detachment induces the activation of autophagy, which acts as a negative regulator of apoptosis (Besirli et al., 2011).

Despite the presence of a retinal vasculature, photoreceptors become hypoxic during periods of retina-RPE separation (Linsenmeier, 1990; Mervin et al., 1999). Physiologically, this is not surprising, as the photoreceptors receive their nutritional support from the choroidal circulation via the RPE. In animal models of retinal detachment, it has been shown that supplemental oxygen can limit photoreceptor cell death and secondary morphologic changes in the retina, presumably by increasing the oxygen tension in the outer retina (Lewis et al., 1999; Mervin et al., 1999; Stone et al., 1999). Still unknown, however, are the molecular events that occur within the retina, and the photoreceptors, in particular, in response to hypoxia. In this study, we showed that the detachment-induced hypoxia of photoreceptors activates autophagy through a HIF-1α mediated pathway. Silencing of HIF-1α reduces the extent of autophagy and shifts cells toward cell death. Together these results point toward the critical role of HIF-1α as an upstream signaler of photoreceptor hypoxia and as an initiator of autophagy as an early pro-survival pathway for these cells.

Studies of hypoxia-induced autophagy in alternative cell systems have shown that hypoxia induces protein expression of HIF-1α which leads to the transcription of the target gene BNIP3 that competes with Bcl-2 and Bcl-X_L for interaction with Beclin to induce autophagy (Bellot et al., 2009; Mazure and Pouyssegur, 2009; Zhang et al., 2008). Detached retinas and hypoxic 661W photoreceptor cells showed increased expression of BNIP3 following induction of HIF-1α expression. These results suggest that a similar mechanism is occurring in the retina following retinal detachment.

Studies in non-ocular tissue suggest that both HIF-1α and HIF-2α are involved in the hypoxia-induced activation of autophagy (Bellot et al., 2009). Though we detect increased levels of HIF-1α and HIF-2α in the retina post-detachment, our current data supports a distinct mechanism which involves HIF-1α, but not HIF-2α in the activation of autophagy within photoreceptors. This observation reveals that a different mechanism may be occurring in the retina in which HIF-1α and HIF-2α perform distinct roles. It is known that HIF-1α and HIF-2α have unique transcriptional targets. Previous gene microarray analyses of the transcriptional profile of detached retinas have shown the increased expression of HIF-activated genes including: annexin A2, heme oxygenase 1, hexokinase, and thioredoxin interacting protein (Hu et al., 2003; Patel and Simon, 2008; Raval et al., 2005). We are currently investigating the specific pathways activated by these two transcription factors in response to retina-RPE separation.

Previous studies from our group have demonstrated that activation of Fas death receptor can induce autophagy in cultured photoreceptor cells (Besirli et al., 2011). In addition, the Fas receptor was also found to be active in detached retinas at 3 and 7 days post detachment, suggesting that Fas induction of autophagy functions to autoregulate Fas-mediated apoptosis (Zacks et al., 2004). The current study has identified that HIF-1α-induced autophagy occurs as early as 1 day post detachment. These data together suggest that the hypoxic response of

the cells through HIF-1α occur early to induce autophagy, whereas Fas-induced autophagy may be later and occur after 3 days of detachment. This observation is expected due to the existence of the hypoxic environment immediately following detachment and delayed activation of the Fas receptor. Further experiments are needed to identify the mechanism of Fas-induced autophagy following retinal detachment and to identify the point at which autophagy switches from being hypoxia-induced to Fas-induced.

While in other systems, HIF-2α can activate autophagy, we did not find that to be the case in our model of photoreceptor hypoxia during retinal detachment. HIF-1α and HIF-2α are known to have distinct targets, and as such it is possible that in the context of retinal detachment, HIF-2α may initiate a unique set of signaling pathways, different from that activated by HIF-1α. One intriguing possibility is that HIF-2α activates transcription of Fas itself. Studies in chondrocytes have shown that HIF-2α regulates the expression of catabolic genes involved in osteoarthritic cartilage destruction (Yang et al., 2010), and that there are three HIF-2α binding sites on the Fas promoter that allow for HIF-2α regulation of Fas expression (Ryu et al., 2012). We are currently testing the hypothesis that hypoxic induction of HIF-2α expression following retina-RPE separation could be responsible for the detachment-induced activation of Fas expression.

In summary, our findings demonstrate that the early activation of autophagy following retinal detachment is mediated by hypoxia. The detachment results in a hypoxic environment for the photoreceptors that initiates a cellular response through hypoxia-inducible factor 1α, which initiates autophagy via a mechanism involving BNIP3. This defined pathway has added a new dimension to our understanding of signaling pathways utilized post retinal injury in a model of retinal detachment.

Acknowledgements

References

al-Ubaidi MR, Font RL, Quiambao AB, Keener MJ, Liou GI, Overbeek PA, Baehr W. Bilateral retinal and brain tumors in transgenic mice expressing simian virus 40 large T antigen under control of the human interphotoreceptor retinoid-binding protein promoter. J Cell Biol. 1992; 119:1681–1687. [PubMed: 1334963]

Al-Ubaidi MR, Matsumoto H, Kurono S, Singh A. Proteomics profiling of the cone photoreceptor cell line, 661W. Adv Exp Med Biol. 2008; 613:301–311. [PubMed: 18188958]

Ban Y, Rizzolo LJ. Regulation of glucose transporters during development of the retinal pigment epithelium. Brain Res Dev Brain Res. 2000; 121:89–95. [PubMed: 10837896]

Barth S, Glick D, Macleod KF. Autophagy: assays and artifacts. J Pathol. 2010; 221:117–124. [PubMed: 20225337]

Bellot G, Garcia-Medina R, Gounon P, Chiche J, Roux D, Pouyssegur J, Mazure NM. Hypoxia-induced autophagy is mediated through hypoxia-inducible factor induction of BNIP3 and BNIP3L via their BH3 domains. Mol Cell Biol. 2009; 29:2570–2581. [PubMed: 19273585]

Benita Y, Kikuchi H, Smith AD, Zhang MQ, Chung DC, Xavier RJ. An integrative genomics approach identifies Hypoxia Inducible Factor-1 (HIF-1)-target genes that form the core response to hypoxia. Nucleic Acids Res. 2009; 37:4587–4602. [PubMed: 19491311]

Besirli CG, Chinskey ND, Zheng QD, Zacks DN. Inhibition of retinal detachment-induced apoptosis in photoreceptors by a small peptide inhibitor of the fas receptor. Invest Ophthalmol Vis Sci. 2010; 51:2177–2184. [PubMed: 19850829]

Besirli CG, Chinskey ND, Zheng QD, Zacks DN. Autophagy activation in the injured photoreceptor inhibits fas-mediated apoptosis. Invest Ophthalmol Vis Sci. 2011; 52:4193–4199. [PubMed: 21421874]

Besirli CG, Zheng QD, Reed DM, Zacks DN. ERK-mediated activation of Fas apoptotic inhibitory molecule 2 (Faim2) prevents apoptosis of 661W cells in a model of detachment-induced photoreceptor cell death. PLoS One. 2012; 7:e46664. [PubMed: 23029562]

Brahimi-Horn MC, Pouyssegur J. HIF at a glance. J Cell Sci. 2009; 122:1055–1057. [PubMed: 19339544]

Burton TC. Recovery of visual acuity after retinal detachment involving the macula. Trans Am Ophthalmol Soc. 1982; 80:475–497. [PubMed: 6763802]

Chong D, Boehlke CS, Zheng QD, Zhang L, Han Y, Zacks DN. Interleukin-6 as a photoreceptor neuroprotectant in an experimental model of retinal detachment. Invest Ophthalmol Vis Sci. 2008

Cook B, Lewis GP, Fisher SK, Adler R. Apoptotic photoreceptor degeneration in experimental retinal detachment. Invest Ophthalmol Vis Sci. 1995; 36:990–996. [PubMed: 7730033]

Greer SN, Metcalf JL, Wang Y, Ohh M. The updated biology of hypoxia-inducible factor. Embo J. 2012; 31:2448–2460. [PubMed: 22562152]

Hisatomi T, Sakamoto T, Goto Y, Yamanaka I, Oshima Y, Hata Y, Ishibashi T, Inomata H, Susin SA, Kroemer G. Critical role of photoreceptor apoptosis in functional damage after retinal detachment. Curr Eye Res. 2002; 24:161–172. [PubMed: 12221523]

Hu CJ, Wang LY, Chodosh LA, Keith B, Simon MC. Differential roles of hypoxia-inducible factor 1alpha (HIF-1alpha) and HIF-2alpha in hypoxic gene regulation. Mol Cell Biol. 2003; 23:9361–9374. [PubMed: 14645546]

Jiang BH, Rue E, Wang GL, Roe R, Semenza GL. Dimerization, DNA binding, and transactivation properties of hypoxia-inducible factor 1. J Biol Chem. 1996; 271:17771–17778. [PubMed: 8663540]

Kong X, Alvarez-Castelao B, Lin Z, Castano JG, Caro J. Constitutive/hypoxic degradation of HIF-alpha proteins by the proteasome is independent of von Hippel Lindau protein ubiquitylation and the transactivation activity of the protein. J Biol Chem. 2007; 282:15498–15505. [PubMed: 17403672]

Lewis G, Mervin K, Valter K, Maslim J, Kappel PJ, Stone J, Fisher S. Limiting the proliferation and reactivity of retinal Muller cells during experimental retinal detachment: the value of oxygen supplementation. Am J Ophthalmol. 1999; 128:165–172. [PubMed: 10458171]

Li QF, Wang XR, Yang YW, Lin H. Hypoxia upregulates hypoxia inducible factor (HIF)-3alpha expression in lung epithelial cells: characterization and comparison with HIF-1alpha. Cell Res. 2006; 16:548–558. [PubMed: 16775626]

Linsenmeier RA. Electrophysiological consequences of retinal hypoxia. Graefes Arch Clin Exp Ophthalmol. 1990; 228:143–150. [PubMed: 2338252]

Maiuri MC, Criollo A, Tasdemir E, Vicencio JM, Tajeddine N, Hickman JA, Geneste O, Kroemer G. BH3-only proteins and BH3 mimetics induce autophagy by competitively disrupting the interaction between Beclin 1 and Bcl-2/Bcl-X(L). Autophagy. 2007; 3:374–376. [PubMed: 17438366]

Mazure NM, Pouyssegur J. Atypical BH3-domains of BNIP3 and BNIP3L lead to autophagy in hypoxia. Autophagy. 2009; 5:868–869. [PubMed: 19587545]

Mazure NM, Pouyssegur J. Hypoxia-induced autophagy: cell death or cell survival? Curr Opin Cell Biol. 2010; 22:177–180. [PubMed: 20022734]

Mervin K, Valter K, Maslim J, Lewis G, Fisher S, Stone J. Limiting photoreceptor death and deconstruction during experimental retinal detachment: the value of oxygen supplementation. Am J Ophthalmol. 1999; 128:155–164. [PubMed: 10458170]

Mizushima N, Yoshimori T, Levine B. Methods in mammalian autophagy research. Cell. 2010; 140:313–326. [PubMed: 20144757]

Patel SA, Simon MC. Biology of hypoxia-inducible factor-2alpha in development and disease. Cell Death Differ. 2008; 15:628–634. [PubMed: 18259197]

Peterson GL. A simplification of the protein assay method of Lowry et al. which is more generally applicable. Anal Biochem. 1977; 83:346–356. [PubMed: 603028]

Piccolino FC, de la Longrais RR, Ravera G, Eandi CM, Ventre L, Abdollahi A, Manea M. The foveal photoreceptor layer and visual acuity loss in central serous chorioretinopathy. Am J Ophthalmol. 2005; 139:87–99. [PubMed: 15652832]

Pouyssegur J, Dayan F, Mazure NM. Hypoxia signalling in cancer and approaches to enforce tumour regression. Nature. 2006; 441:437–443. [PubMed: 16724055]

Raval RR, Lau KW, Tran MG, Sowter HM, Mandriota SJ, Li JL, Pugh CW, Maxwell PH, Harris AL, Ratcliffe PJ. Contrasting properties of hypoxia-inducible factor 1 (HIF-1) and HIF-2 in von Hippel-Lindau-associated renal cell carcinoma. Mol Cell Biol. 2005; 25:5675–5686. [PubMed: 15964822]

Ross WH. Visual recovery after macula-off retinal detachment. Eye (Lond). 2002; 16:440–446. [PubMed: 12101451]

Ross WH, Kozy DW. Visual recovery in macula-off rhegmatogenous retinal detachments. Ophthalmology. 1998; 105:2149–2153. [PubMed: 9818620]

Ross WH, Stockl FA. Visual recovery after retinal detachment. Curr Opin Ophthalmol. 2000; 11:191–194. [PubMed: 10977226]

Rouschop KM, Wouters BG. Regulation of autophagy through multiple independent hypoxic signaling pathways. Curr Mol Med. 2009; 9:417–424. [PubMed: 19519399]

Ryu JH, Shin Y, Huh YH, Yang S, Chun CH, Chun JS. Hypoxia-inducible factor-2alpha regulates Fas-mediated chondrocyte apoptosis during osteoarthritic cartilage destruction. Cell Death Differ. 2012; 19:440–450. [PubMed: 21869830]

Sarkar S, Perlstein EO, Imarisio S, Pineau S, Cordenier A, Maglathlin RL, Webster JA, Lewis TA, O'Kane CJ, Schreiber SL, et al. Small molecules enhance autophagy and reduce toxicity in Huntington's disease models. Nat Chem Biol. 2007; 3:331–338. [PubMed: 17486044]

Stone J, Maslim J, Valter-Kocsi K, Mervin K, Bowers F, Chu Y, Barnett N, Provis J, Lewis G, Fisher SK, et al. Mechanisms of photoreceptor death and survival in mammalian retina. Prog Retin Eye Res. 1999; 18:689–735. [PubMed: 10530749]

Strauss O. The retinal pigment epithelium in visual function. Physiol Rev. 2005; 85:845–881. [PubMed: 15987797]

Tan E, Ding XQ, Saadi A, Agarwal N, Naash MI, Al-Ubaidi MR. Expression of cone-photoreceptor-specific antigens in a cell line derived from retinal tumors in transgenic mice. Invest Ophthalmol Vis Sci. 2004; 45:764–768. [PubMed: 14985288]

Tracy K, Dibling BC, Spike BT, Knabb JR, Schumacker P, Macleod KF. BNIP3 is an RB/E2F target gene required for hypoxia-induced autophagy. Mol Cell Biol. 2007; 27:6229–6242. [PubMed: 17576813]

Verardo MR, Lewis GP, Takeda M, Linberg KA, Byun J, Luna G, Wilhelmsson U, Pekny M, Chen DF, Fisher SK. Abnormal reactivity of muller cells after retinal detachment in mice deficient in GFAP and vimentin. Invest Ophthalmol Vis Sci. 2008; 49:3659–3665. [PubMed: 18469190]

Wang GL, Jiang BH, Rue EA, Semenza GL. Hypoxia-inducible factor 1 is a basic-helix-loop-helix-PAS heterodimer regulated by cellular O2 tension. Proc Natl Acad Sci U S A. 1995; 92:5510–5514. [PubMed: 7539918]

Wang GL, Semenza GL. Purification and characterization of hypoxia-inducible factor 1. J Biol Chem. 1995; 270:1230–1237. [PubMed: 7836384]

Wu D, Yotnda P. Induction and testing of hypoxia in cell culture. J Vis Exp. 2011

Yang S, Kim J, Ryu JH, Oh H, Chun CH, Kim BJ, Min BH, Chun JS. Hypoxia-inducible factor-2alpha is a catabolic regulator of osteoarthritic cartilage destruction. Nat Med. 2010; 16:687–693. [PubMed: 20495569]

Zacks DN, Boehlke C, Richards AL, Zheng QD. Role of the Fas-signaling pathway in photoreceptor neuroprotection. Arch Ophthalmol. 2007; 125:1389–1395. [PubMed: 17923548]

Zacks DN, Hanninen V, Pantcheva M, Ezra E, Grosskreutz C, Miller JW. Caspase activation in an experimental model of retinal detachment. Invest Ophthalmol Vis Sci. 2003; 44:1262–1267. [PubMed: 12601057]

Zacks DN, Zheng QD, Han Y, Bakhru R, Miller JW. FAS-mediated apoptosis and its relation to intrinsic pathway activation in an experimental model of retinal detachment. Invest Ophthalmol Vis Sci. 2004; 45:4563–4569. [PubMed: 15557468]

Zhang H, Bosch-Marce M, Shimoda LA, Tan YS, Baek JH, Wesley JB, Gonzalez FJ, Semenza GL. Mitochondrial autophagy is an HIF-1-dependent adaptive metabolic response to hypoxia. J Biol Chem. 2008; 283:10892–10903. [PubMed: 18281291]

Highlights

- Retinal detachment induces an increase in HIF-1α and HIF-2α protein levels.

- HIF-1α protein levels are increased in hypoxic 661W photoreceptor cells

- Increased HIF-1α in cells and detached retina causes increased BNIP3 and LC3-II.

- Silencing of HIF-1α in cells and detached retina increased apoptotic cell death.
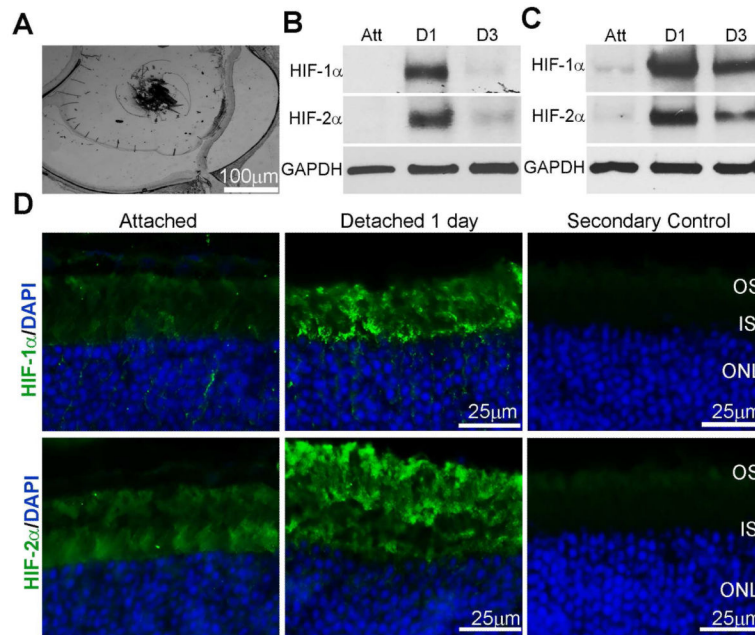
**Fig. 1. HIF-1α and HIF-2α are expressed in attached and detached rat retinas**
(A) Light micrograph of a cryosection from detached retina at 1 day post detachment. **(B-C)** HIF-1α and HIF-2α protein immunoreactivity on western blots of attached or detached mouse and rat retina protein homogenates, respectively. Samples were collected at 1 and 3 days post detachment. GAPDH served as a loading control. Att, attached retina; D1, 1 day detached retinas; D3, 3 day detached retinas, n=3 animals per time point. **(D)** HIF-1α and HIF-2α localization on attached and 1 day detached retina cross-sections from C57BL/6J mice with immunohistochemical analysis. Control sections from which primary antibodies are omitted are shown. OS, outer segments; IS, inner segments; ONL, outer nuclear layer.
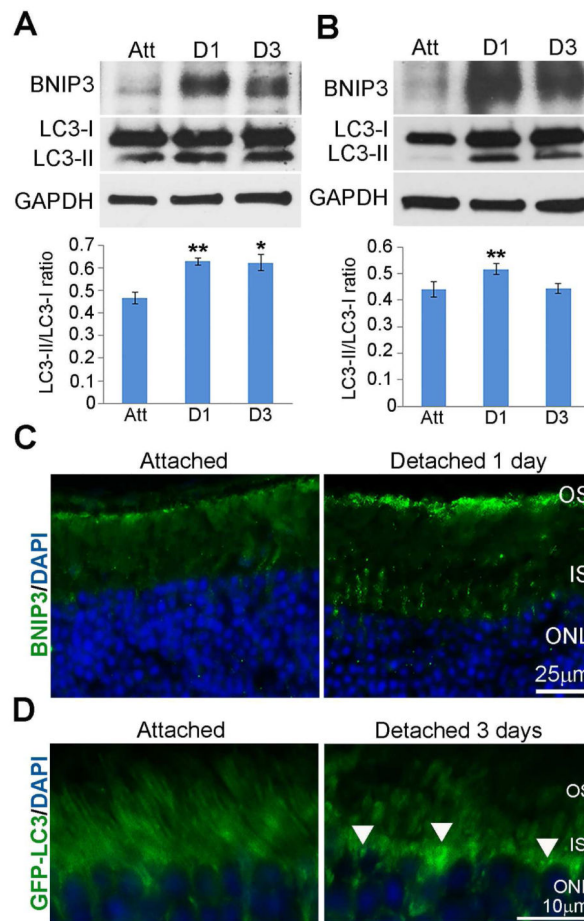
Fig. 2. BNIP3 and LC3 expression in detached rat retinas correlates with HIF-1α and HIF-2α expression

(A-B) BNIP3 and LC3 protein immunoreactivity on western blots of attached or detached mouse or rat retina protein homogenates, respectively. Samples were collected at 1 and 3days post detachment. GAPDH served as a loading control. The ratios of LC3-II to LC3-I levels were based on densitometry of respective bands from western blots are shown. Att, attached retina; D1, 1 day detached retinas; D3, 3 day detached retinas. **(A)** The ratios at 1 and 3 days post-detachment were significantly higher than attached mice retinas (p** < 0.005, p*<0.05, n=3 animals per time point). **(B)** The ratio at 1 day post-detachment is significantly higher than the attached rat retinas (n=3 animals per time point, p**<0.005, ANOVA followed by Bonferroni's test). **(C)** Representative images of BNIP3 immunohistochemical localization on attached and 1 day detached retinas from C57BL/6 mice counter-stained with DAPI. **(D)** LC3 localization on attached and 1 day detached GFP-LC3 mouse retina cross-sections. Arrows indicate punctate like structures. OS, outer segments; IS, inner segments; ONL, outer nuclear layer.
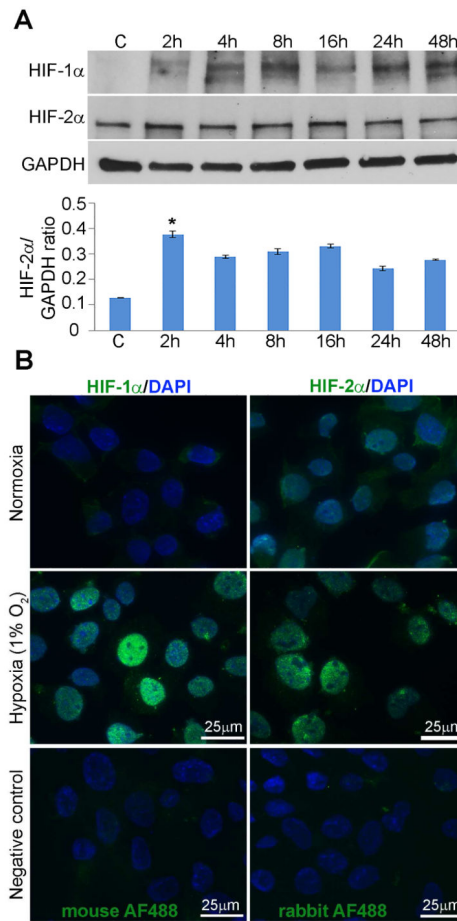
Fig. 3. Hypoxia induces HIF-1α and HIF-2α expression in 661W photoreceptor cells
(**A**) HIF-1α and HIF-2α protein immunoreactivity on western blots of homogenates from 661W cells incubated in normoxic conditions or hypoxic (1% O_2, 5% CO_2, 94% N_2) conditions over times indicated. GAPDH served as a loading control. The ratios of HIF-2α and GAPDH levels based on densitometry of respective bands from western blots are shown. Control sample, C, were from cells grown in normoxic conditions. Images are representative of 9 independent experiments with cells between passages 4 and 6. The overall effect of hypoxia on HIF-2α protein levels was assessed by ANOVA followed by Bonferroni's test $p < 0.05$. (**B**) Immunohistochemical analysis of cultured 661W photoreceptor cells under hypoxic conditions for 24 hours and normoxic controls. Cells were fixed and stained with antibodies recognizing HIF-1α or HIF-2α. DAPI-stained nuclei are shown in blue. Control images of cells from which primary antibodies are omitted are shown.
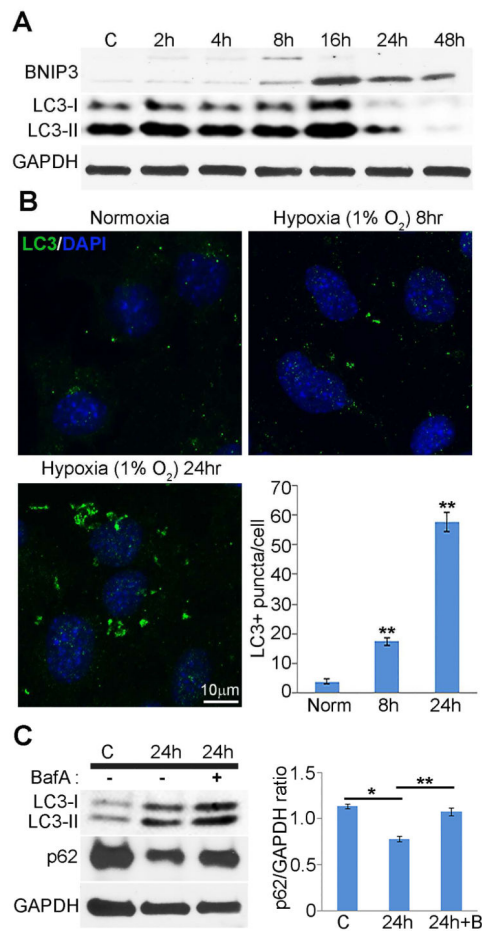
Fig. 4. Hypoxia induces autophagy in 661W photoreceptor cells

Western and immunohistochemical analysis of LC3 protein in 661W cells under hypoxic conditions. **(A)** LC3 and BNIP3 protein immunoreactivity on western blots of homogenates from 661W incubated in normoxic or hypoxic conditions for times indicated. C, control normoxic sample. Quantification of LC3-II/GAPDH ratios was based on densitometry measurements of western blots. The level of LC3-II has a significant peak 16 hours hypoxia (p **< 0.005). Images are representative of 9 independent experiments with cells between passage 4 and 6. **(B)** 661W cells were incubated in hypoxic conditions for 8 or 24 hours post confluence, fixed, and stained with antibody against LC3. DAPI-stained nuclei are shown in blue. The number of LC3+ punctae/cell was quantified at times indicated (bar graphs). Error bars represent mean ± SEM, n=3 independent experiments using 9 non-overlapping fields of 100 μm for each condition. p values were calculated using ANOVA followed by Bonferroni's test, and are as shown: p**<0.005. **(C)** 661W cells were cultured under normoxic or hypoxic conditions for 24 hours in the presence or absence of Bafilomycin A, an inhibitor of autophagic vacuole maturation for the last 4 hours of the incubation and evaluated by western analysis with antibodies recognizing LC3 and p62. Ratios of p62/GAPDH are shown that are representative of 3 independent experiments.
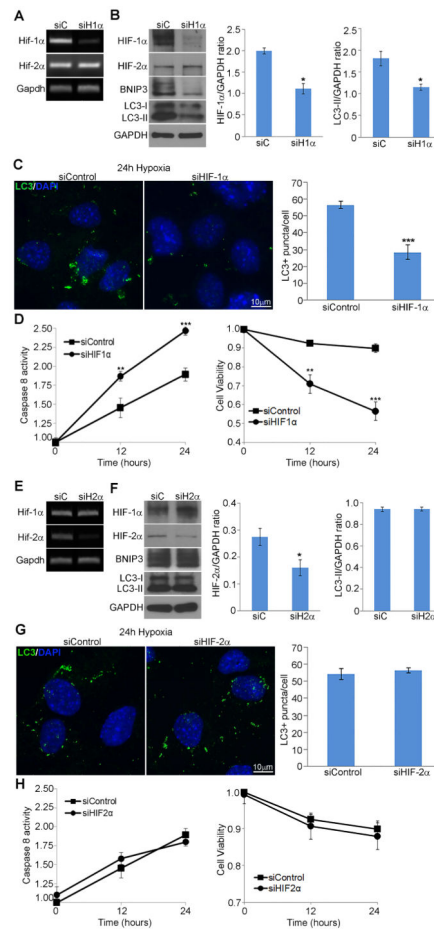
Fig. 5. HIF-1α but not HIF-2α is required for hypoxia-induced autophagy in 661W photoreceptor cells

(A-D) 661W cells were transfected with a pool of HIF-1α targeting siRNAs or a non-targeting siRNA control pool, and incubated in hypoxic conditions for 16 or 24 hours post confluence. **(A)** Transcript expression for Hif-1α, Hif-2α, and Gapdh evaluated using RT-PCR. **(B)** Protein levels of HIF-1α, HIF-2α, BNIP3, LC3, and GAPDH evaluated by western blot analysis of 661W cell homogenates lysed after 16 hours of hypoxia. Ratios of HIF-1α/GAPDH show a significant decrease of HIF-1α expression following treatment with siHIF-1α (p*<0.05). Ratios of LC3-II/GAPDH show a significant decrease in LC3-II in the presence of siHIF-1α (p*<0.05). Blots are representative of 3 independent experiments. Comparison of LC3-II to GAPDH was utilized due to the variability of LC3-I levels in cultured cells. **(C)** Immunohistochemical analysis of representative fields of 661W cells with LC3B punctae labeled in green and DAPI-stained nuclei shown in blue. The number of LC3+ punctae/cell was quantified after hypoxic incubation for 24 hours (bar graphs). Error bars represent mean ± SEM, n=3 independent experiments using 9 non-overlapping fields of 100 μm for each condition (p***<0.0005). **(D)** Caspase 8 activation and cell viability was evaluated following hypoxia for times indicated, n = 3 independent experiments using 9 non-overlapping fields of 100 μm for each condition (p**<0.005, p*** <0.0005, Student's *t*-test). **(E-H)** 661W cells were transfected with a pool of HIF-2α targeting siRNAs or a non-
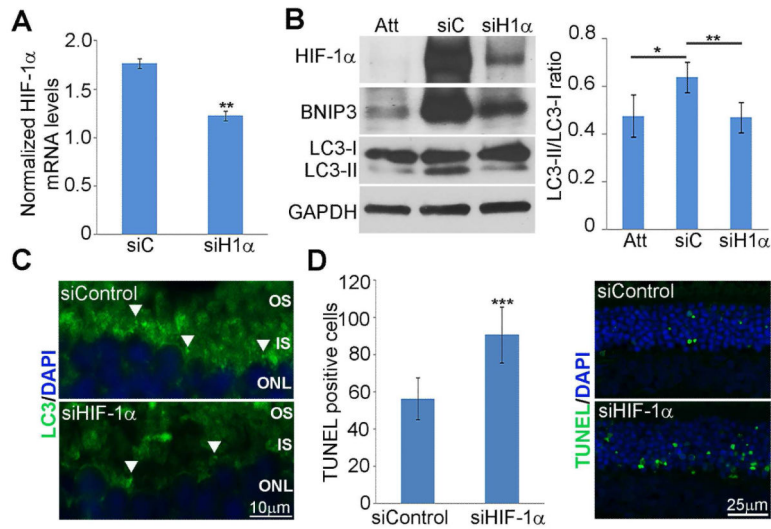
targeting siRNA control pool, incubated in hypoxic conditions for 16 or 24 hours post confluence and evaluated as in A-D.

Fig. 6. Silencing of HIF-1α in detached retinas increases cell death and decreases autophagy
Retinal detachments were created in rats and siRNA against HIF-1α or Non-targeting controls were introduced into the subretinal space immediately following detachment. **(A)** Transcript expression for HIF-1α at 1 day post detachment evaluated using qRT-PCR. Ratios represent fold change in relation to attached control retinas in same animals. Error bars represent mean ± SEM, n=3 animals. p**<0.005. **(B)** Protein levels of HIF-1α, BNIP3, and LC3 evaluated by western blot analysis of retinal homogenates. Immunoblots shown are representative of three sets of animals. GAPDH served as a loading control. Densitometry ratios of the LC3-II/LC3-I bands are shown. Animals treated with siHIF-1α showed a significant decrease in LC3-II/LC3-I ratios in relation to animals treated with siControl (p**<0.005, n = 3 animals). **(C)** LC3 localization on cross-sections from rat retinas detached and treated with siRNA against HIF-1α or Non-targeting controls with immunohistochemical analysis. Arrows indicate punctate like structures. OS, outer segments; IS, inner segments; ONL, outer nuclear layer. **(D)** TUNEL staining of 3 day detached retinas treated with siRNA against HIF-1α or Non-targeting controls. Bar graph depicts number of TUNEL positive cells per 40X viewing field in the outer nuclear layer. Error bars represent mean ± SEM, n=3 animals with quantification of 9 non-overlapping fields of 300 μm per retina (p***<0.0005, Student's *t*-test).